Published online 11 November 2017

Nucleic Acids Research, 2018, Vol. 46, No. 2 ***e12***
doi: 10.1093/nar/gkx1086

A bacterial three-hybrid assay detects *Escherichia coli* Hfq–sRNA interactions *in vivo*

Katherine E. Berry* **and Ann Hochschild***

Department of Microbiology and Immunobiology, Harvard Medical School, Boston, MA 02115, USA

Received August 03, 2017; Revised September 21, 2017; Editorial Decision October 14, 2017; Accepted October 20, 2017

ABSTRACT

The interaction of RNA molecules with proteins is a critical aspect of gene regulation across all domains of life. Here, we report the development of a bacterial three-hybrid (B3H) assay to genetically detect RNA–protein interactions. The basis for this three-hybrid assay is a transcription-based bacterial two-hybrid assay that has been used widely to detect and dissect protein–protein interactions. In the three-hybrid assay, a DNA-bound protein with a fused RNA-binding moiety (the coat protein of bacteriophage MS2 ($MS2^{CP}$)) is used to recruit a hybrid RNA upstream of a test promoter. The hybrid RNA consists of a constant region that binds the tethered $MS2^{CP}$ and a variable region. Interaction between the variable region of the hybrid RNA and a target RNA-binding protein that is fused to a subunit of *Escherichia coli* RNA polymerase (RNAP) stabilizes the binding of RNAP to the test promoter, thereby activating transcription of a reporter gene. We demonstrate that this three-hybrid assay detects interaction between non-coding small RNAs (sRNAs) and the hexameric RNA chaperone Hfq from *E. coli* and enables the identification of Hfq mutants with sRNA-binding defects. Our findings suggest that this B3H assay will be broadly applicable for the study of RNA–protein interactions.

INTRODUCTION

RNA–protein interactions are ubiquitous in biology and play critical roles in gene expression across all domains of life, regulating transcription, translation and turnover of messenger RNA (mRNA). A variety of assays have been developed to facilitate the identification of RNA-binding proteins and their RNA ligands and to probe the nature of these interactions (1–11). The functional understanding of an RNA–protein interaction of interest typically depends on an ability to disrupt or otherwise perturb that interaction, enabling a phenotypic analysis of the consequences of such perturbation. Accordingly, the development of genetic tools that can both detect RNA–protein interactions and also facilitate the identification of perturbing mutations is a priority.

Trans-acting small RNAs (sRNAs) that function as regulators are present throughout the bacterial domain of life. These sRNAs, which commonly affect the translation and/or stabilities of target mRNAs via imperfect base-pairing interactions, influence all aspects of bacterial physiology, including the response to nutritional and other stresses (reviewed in (12–14)). Many of these sRNAs depend on interactions with specific proteins for their function, the best characterized of which is the sRNA chaperone Hfq originally identified in *Escherichia coli* (15). A homohexameric Lsm-like protein, Hfq has orthologs in approximately half of sequenced bacterial species (16–18). As well as increasing the half-lives of many sRNAs, Hfq facilitates sRNA–mRNA base-pairing through simultaneous interaction with sRNAs and their mRNA targets. Specifically, Hfq binds sRNA–mRNA pairs through contacts with three distinct surfaces of its toroid-like structure: (i) the proximal face binds polyU sequences in the intrinsic terminators of sRNAs; (ii) the distal face binds $(ARN)_x$ motifs often found in mRNA targets; (iii) the rim surface interacts with AU rich sequences (reviewed in (14)). In bringing together sRNAs and their mRNA targets, Hfq can ensure the appropriate translational regulation, but can also trigger mRNA degradation (sometimes in the absence of any translational effect) via the recruitment of cellular endonucleases such as RNase E (reviewed in (12,19)). Hfq-dependent effects of sRNAs on transcription termination have also been reported, implying co-transcriptional binding to target mRNAs (20,21).

Here, we build on a well-established transcription-based bacterial two-hybrid (B2H) assay for detecting protein–protein interactions to develop a bacterial three-hybrid assay (B3H) that detects RNA–protein interactions. We establish the utility of the B3H assay by examining the interactions between *E. coli* Hfq and its associated sRNAs. We show further that this B3H assay enables the facile identification of Hfq mutants with specific defects in their abilities to bind sRNA ligands when used in tandem with a B2H as-

*To whom correspondence should be addressed. Tel: +1 617 432 1986; Fax: +1 617 738 7664; Email: ann_hochschild@hms.harvard.edu
Correspondence may also be addressed to Katherine E. Berry. Tel: +1 413 538 3262; Fax: +1 413 538 2327; Email: kberry@mtholyoke.edu
Present address: Katherine E Berry. Department of Chemistry, Mount Holyoke College, South Hadley, MA 01075, USA.

say that detects the Hfq self-interaction and can therefore be used to discard Hfq mutants that are misfolded and/or unstably produced. The establishment of a three-hybrid assay using bacterial cells offers potential to expand the range of RNA–protein interactions that can be investigated genetically. In particular, our B3H assay provides a complement to established yeast three-hybrid assays for studying RNA–protein interactions (1,2,8,22); as well as offering high transformation efficiency, the *E. coli*-based system enables the production of hybrid RNAs with bacterial intrinsic terminators at their 3′ ends, which cannot be produced in yeast. We anticipate that our bacterial system will facilitate the study of diverse RNA-binding proteins from bacteria and other organisms.

MATERIALS AND METHODS

Bacterial strains and plasmids

A complete list of plasmids, strains and oligonucleotides (oligos) used in this study is provided in Supplemental Tables S1–3, respectively. NEB 5-α F'I^q cells (New England Biolabs) were used as the recipient strain for all plasmid constructions.

Escherichia coli strain KB460 was constructed by replacing the *Hfq* open reading frame (ORF) of MG1655 with a chloramphenicol resistance gene using a previously described protocol (23); linear DNA for λ red recombination was amplified from pKD3 with oligos oKB1154 and oKB1171. Subsequently, this *Δhfq::cam* allele was moved into FW102 O_L2 reporter cells by P1 transduction to make strain KB464. The chloramphenicol resistance allele in strain KB464 was subsequently excised via FLP recombinase expressed from the plasmid pCP20 as described (23) to generate strain KB473.

Escherichia coli strain KB496 is a derivative of FW102 into which the *Δhfq::kan* allele from the Keio collection (24) was inserted via P1 transduction. Single copy *mRNA–lacZ* reporters on F' episomes (bearing tetracycline resistance) were generated as previously described (25,26) by conjugative delivery of pFW11-derivative plasmids pKB1074, pKB1075 and pKB1076 into FW102 cells to yield strains KB515, KB516 and KB517, respectively. The recombinant F' episomes in each strain were then moved via conjugation into *Δhfq* strain KB496 to give *mRNA–lacZ Δhfq* reporter strains KB519, KB521 and KB522, respectively.

Plasmids were constructed as specified in Table S1 and the construction of key parent vectors is described below. pKB822 (pCDF–pBAD) carries the origin and spectinomycin resistance gene from plasmid pCDF1b, and the *araC-pBAD-rrnB* sequences from pBAD33. To create pKB822, the PCR product of primers oKB1044 + oKB1045 on pBAD33 containing *araC-pBAD-rrnB* was digested with Bsu36I and NarI, and ligated with a pCDF1b vector backbone digested at the same restriction sites. pKB845 (pCDF–pBAD–2x$MS2^{hp}$–XmaI–HindIII) was derived from pKB822 by digestion of the vector with BamHI and HindIII followed by ligation of an insert, encoding two MS2 RNA hairpins (2x$MS2^{hp}$) and an XmaI site, that was formed by the overlap polymerase chain reaction (PCR) product of oKB1132 + oKB1129 on pKB822 and oKB1128 + oKB1133 on pIIIA/MS2–2 (27). All 2X$MS2^{hp}$–sRNA hybrids were constructed by inserting the sRNA of interest into the XmaI/HindIII sites of pKB845. No terminator sequence outside of the intrinsic terminators in each sRNA was provided, except for a *trpA* terminator in pKB1094, downstream of the 2x$PP7^{hp}$ sequence. pKB989 (pACλCI–$MS2^{CP}$) expresses a fusion between λ CI protein (λCI) and a mutant MS2 coat protein ($MS2^{CP}$) containing V30I, A81G, Δ68–80 (deleted 68-VATQTVGGVELPV-80); these mutations minimize MS2 multimerization (28). This $MS2^{CP}$ sequence was fused to the C-terminus of λCI, after a 12-aa linker (AAAEFPGIHPGM; adapted from (22)). pKB817 (pBRα–Hfq) contains full-length *E. coli* Hfq fused to the α-NTD (residues 1–248), downstream of a three-alanine linker. This insert was cloned into pBRα between NotI and BamHI sites.

β-galactosidase assays

B2H/B3H assays. For B3H assays, reporter cells (WT FW102 OL_2–62 or *Δhfq* strain KB473) were freshly co-transformed with compatible pAC, pBR and pCDF derived plasmids, as indicated. To maintain consistent growth conditions between B3H and B2H assays, an empty pCDF vector (pKB822) was included in B2H assays. From each transformation three colonies were picked into 1 ml LB broth supplemented with carbenicillin (50 μg/ml), chloramphenicol (25 μg/ml), kanamycin (50 μg/ml), spectinomycin (100 μg/ml) and 0.2% arabinose in a 2 ml 96-well deep well block (Axygen, Corning), sealed with breathable film and shaken at 900 rpm with 80% humidity in a Multitron 2000 shaking incubator (Infors HT) for ∼16 h. Overnight cultures were diluted 1:50 into 200 μl LB supplemented as above, with an additional 5 μM isopropyl-β-D-thiogalactoside (IPTG), unless otherwise noted. Cells were grown to mid-log in optically clear 200 μl flat bottom 96-well plates (Greiner) covered with plastic lids, as above. Cells were lysed and β-galactosidase activity was measured as previously described (29). B3H and B2H interactions (except in Figure 1) are reported as the fold-stimulation over basal levels; this is the β-galactosidase activity in reporter cells containing all hybrid constructs (α-X, λCI-$MS2^{CP}$ and $MS2^{hp}$-Z for the B3H and α-X, λCI-Y for the B2H), divided by the highest activity from negative controls—cells containing plasmids where one of the hybrid constructs is replaced by an α empty, λCI empty or $MS2^{hp}$ empty construct. Assays were conducted in biological triplicate on at least three separate days and a representative dataset is shown. Values shown are averages from one biological triplicate experiment and error bars represent one standard deviation from the mean of these values.

sRNA activity assays. Reporter cells (KB515, KB519, KB516, KB521, KB517 or KB522) were freshly transformed with pBRα, pKB817 or pKB1046. Overnight cultures (1 ml) were grown in triplicate in deep-well plates as for B3H assays, but LB broth was supplemented with tetracycline (10 μg/ml), carbenicillin (50 μg/ml) and IPTG (5 μM). Overnight cultures were diluted in the same medium (200 μl) and subcultures were grown in covered plates as for B3H assays, but to early stationary phase (OD ∼1.0). Cells were lysed and assayed for β-galactosidase activity as above.

Western blots

Cell lysates from β-galactosidase assays were normalized based on pre-lysis OD_{600}. Lysates were mixed with 4× Laemmli loading dye with fresh β-mercaptoethanol, boiled for 10 min at 95°C and electrophoresed on 10–20% Tris-glycine gels (Thermo Fisher) in 1× NuPAGE MES Running Buffer (Thermo Fisher). Proteins were transferred to nitrocellulose membranes (Amersham Protran) using a wet transfer system (Life Technologies), incubated with 1:10,000 primary antibody (α-RpoA-NTD, α-RpoA or α-CI; Neoclone) overnight at 4°C in 1× phosphate-buffered saline (PBS) + 5% milk. Membranes were washed 5× with 1× PBS by rocking at room temperature with ∼20 ml for 5–10 min, and probed with an horseradish peroxidase (HRP)-conjugated secondary antibody (α-mouse IgG or α-rabbit IgG; Cell Signaling, 1:10,000). Chemiluminescent signal from bound peroxidase complexes was detected using ECL Plus western blot detection reagents (GE Healthcare) and a ChemiDock XRS+ imaging system (Bio-Rad) according to manufacturer's instructions.

Northern blots

Cultures for northern blots were grown identically to those for B3H assays above, except that overnight cultures (5 ml) were grown in glass culture tubes. Overnight cultures were back-diluted to $OD_{600} = 0.05$ into 6 ml subcultures in LB and grown to mid-log in a tube roller at 37°C. Cells were pelleted in a micro-centrifuge at 4000 rpm for 2 min at 4°C. Cell pellets from 4 ml of mid-log culture were frozen at −80°C until lysis. To each frozen cell pellet, 1 ml Tri-Reagent (Molecular Research Center) was added. Cells were resuspended by pipetting and lysed by heating at 60°C for 10 min. Lysates were cleared by centrifugation for 10 min at 12,000 rpm at 4°C in a micro-centrifuge. Cleared supernatants were mixed thoroughly with 200 μl chloroform. Samples were allowed to incubate for 5 min at room temperature, then centrifuged for 15 min at 12,000 rpm at 4°C to separate aqueous and organic layers. The aqueous layer (450 μl) was recovered and precipitated by the addition of 100% EtOH (1 ml) and incubation at −80°C overnight. To collect precipitated RNA, samples were centrifuged at maximum speed in a micro-centrifuge at 4°C for 30 min and pellets were washed twice with cold 75% EtOH (800 μl), allowed to air dry and resuspended in water. RNA was quantified by absorbance at 260 nm on a NanoDrop spectrophotometer (Thermo Scientific). On the same day, total RNA samples were prepared for gel electrophoresis following normalization of their concentration by dilution in water. An equal volume of 2× formamide loading dye (95% formamide, 0.025% sodium dodecyl sulphate (SDS), 0.025% bromophenol blue, 0.025% xylene cyanol and 0.025% amaranth) was added and samples were vortexed, heated at 95°C for 3 min and centrifuged for 1 min in a micro-centrifuge prior to loading. RNA was separated on an 8% urea-polyacrylamide gel (National Diagnostics) in 50 mM MOPS, pH 7.0 running buffer. The remainder of the northern blot protocol was conducted as previously described (30), but using standard DNA oligonucleotides (IDT) rather than locked nucleic acid probes. Blots were initially probed for $MS2^{hp}$ hairpins using oKB1301, then stripped by applying three rounds of near-boiling 0.1% SDS (50 ml) and allowing the solution to come to room temperature while rotating in hybridization tubes in a room temperature hybridization oven (each round took ∼15 min). Blots were then reprobed for 5S rRNA with oKB593 as a loading control following the same protocol as initial hybridization.

B3H Screening

A mutant *hfq* library (pKB817, pBRα-Hfq) was generated first by 80 rounds of PCR amplification of the *hfq* portion of the plasmid using Taq DNA Polymerase (GoTaq Green Master Mix, Promega) and primers oKB1077 and oKB1078. The PCR product was digested with DpnI (New England Biolabs) to remove template plasmid, then with NotI-HF and BamHI-HF (New England Biolabs), gel purified and ligated (T4 DNA ligase; New England Biolabs) into a pBRα vector cut with NotI-HF and BamHI-HF. Following ligation and transformation into NEB 5-α $F'I^q$ cells (New England Biolabs), cells were grown as near-lawns on LB-carbenicillin plates and a miniprep was performed from resuspension of ∼30,000 colonies to yield the plasmid library. For the primary screen, the pBRα-Hfq plasmid library was transformed into KB473 cells along with pKB989 (pACλCI-$MS2^{CP}$) and pKB912 (pCDF-$MS2^{hp}$-OxyS) and plated on LB agar supplemented with inducers (0.2% arabinose and 1.5 μM IPTG), antibiotics (carbenicillin (50 μg/ml), chloramphenicol (25 μg/ml), kanamycin (50 μg/ml), and spectinomycin (100 μg/ml)) and indicators (Xgal (40 μg/ml) and phenylethyl-β-D-thiogalactopyranoside (125 μM; Gold Biotech)). Plates were incubated overnight at 37°C, then at 4°C for an additional 4–8 h. Colonies that appeared white or pale from the primary screen were restreaked to confirm colony color. A total of 31 confirmed white/pale colonies were picked and pooled, and plasmid DNA was isolated for use in the secondary screen. For the secondary screen, the miniprep of pooled primary screen hits was transformed into strain KB473 containing pKB816 (pACλCI-$MS2^{CP}$) and pKB845 (pCDF-$MS2^{hp}$-empty). Transformants were plated and grown under the same conditions as the primary screen. Colonies that appeared blue were restreaked to confirm colony color. The pBRα-Hfq plasmid was individually isolated from 36 confirmed blue colonies and the DNA encoding *hfq* was sequenced. Most mutations were isolated multiple times. β-galactosidase assays to confirm and quantify the effects of the eight unique mutations were performed as described above. Each mutant *hfq* sequence was subcloned from the pBRα vector to the pACλCI vector in order to test the effect of the mutation on the B2H Hfq self-interaction when present on *hfq* sequences fused both to α-NTD and to λCI.

RESULTS

Experimental strategy

In the transcription-based B2H assay that served as the basis for developing this B3H assay, contact between a protein domain (X) fused to a subunit of RNAP and a partner domain (Y) fused to a sequence-specific DNA-binding protein activates transcription from a test promoter bearing

an upstream recognition site for the DNA-binding protein (31,32). Here, X is fused to the N-terminal domain of the α subunit of RNAP (α-NTD) and Y is fused to the bacteriophage λ CI protein (λCI) (Figure 1A). A single-copy test promoter contains the λ operator O_L2 centered 62 bp upstream from the transcription start side of a *lacZ* reporter gene (33). In this system, interaction between the DNA-bound λCI fusion protein and the assembled α fusion protein stabilizes the binding of RNAP to the test promoter, thereby activating reporter gene expression. For the envisioned B3H assay, an RNA domain (Z) would be tethered to the upstream O_L2 DNA sequence, using a high-affinity and high-specificity RNA–protein interaction (Figure 1B). We chose to use the bacteriophage MS2 coat protein (hereafter $MS2^{CP}$) for this purpose, which binds as a dimer to a 21 nt RNA hairpin ($MS2^{hp}$) and has been widely used to capture hybrid RNAs, for example in the context of a yeast three-hybrid assay and a bacterial fluorescence complementation assay (1,34).

B3H assay detects an interaction between the PP7 coat protein and its cognate RNA hairpin

As a first test of our strategy, we attempted to detect an interaction between the bacteriophage PP7 coat protein (hereafter $PP7^{CP}$) and its cognate RNA hairpin ($PP7^{hp}$) in cells containing a λCI-$MS2^{CP}$ fusion protein and an α-$PP7^{CP}$ fusion protein (Figure 1C). The PP7-derived components are homologous to the MS2 counterparts, but $PP7^{CP}$ does not bind to the $MS2^{hp}$ RNA, nor does $MS2^{CP}$ bind to the $PP7^{hp}$ RNA (35). We asked whether a hybrid RNA possessing both the $MS2^{hp}$ and the $PP7^{hp}$ was capable of serving as a bridge to link the RNA-binding moieties of the λCI-$MS2^{CP}$ and α-$PP7^{CP}$ fusion proteins (Figure 1C). Indeed, β-galactosidase assays show that transcription from the test promoter was stimulated ∼6-fold when both of these fusion proteins and the full hybrid RNA were present, as compared to the basal activity from the negative controls where any single element ($MS2^{CP}$, $PP7^{CP}$, $MS2^{hp}$ or $PP7^{hp}$) was left out (Figure 1D). Thus, each protein and each RNA element is required to stabilize the binding of RNAP to the test promoter and activate transcription of the *lacZ* reporter gene.

B3H assay detects Hfq–sRNA interaction

To extend our B3H system to a bacterial RNA–protein interaction involved in gene regulation, we sought to detect the interaction of *E. coli* Hfq with one of its interacting sRNAs. We initially chose ChiX as the target sRNA due to its particularly strong binding to Hfq (36,37). We fused Hfq to the α-NTD and created a hybrid RNA possessing two copies of the $MS2^{hp}$ at the 5′ end and one copy the sRNA ChiX at the 3′ end (Figure 1E; only one $MS2^{hp}$ is shown for simplicity). In reporter cells containing both the α-Hfq and λCI-$MS2^{CP}$ fusions proteins along with the MS2–ChiX hybrid RNA, we observed a 6-fold stimulation of β-galactosidase activity over the basal activity level (Figure 1F, top), indicative of an interaction between the Hfq moiety of the α-Hfq fusion protein and the ChiX moiety of the hybrid RNA. We found that this interaction was strengthened in *Δhfq* reporter cells (Figure 1F, bot), likely because endogenous Hfq is no longer present to compete with α-Hfq fusion protein for binding to the hybrid MS2–ChiX RNA. To avoid complications due to the formation of mixed Hfq hexamers comprising both wild-type (WT) and fusion protein subunits, we performed all subsequent experiments in *Δhfq* reporter strain cells, except where the use of the hfq^+ reporter strain is explicitly noted.

As additional controls to ensure that the system was reporting on the Hfq–ChiX interaction as depicted in Figure 1E, we explicitly investigated the contribution of each component interaction to the activation of reporter gene transcription: (i) the protein–DNA interaction of λCI with its operator O_L2, (ii) the protein–RNA interaction of $MS2^{CP}$ with $MS2^{hp}$ RNA and (iii) the protein–RNA interaction of Hfq with ChiX. To do this, we introduced previously characterized single amino acid substitutions into each protein moiety. Specifically, we took advantage of λCI substitution S45A, which disrupts λCI binding to operator DNA (38); $MS2^{CP}$ substitution Y85S, which disrupts the $MS2^{CP}$–$MS2^{hp}$ interaction (39) and Hfq substitution Q8A, which disrupts the interaction of Hfq with most sRNAs (40,41), including ChiX (42). We found that each of these substitutions eliminated the activation of reporter gene expression above the basal levels (Figure 2A). To control for the stabilities of the mutant Hfq and $MS2^{CP}$ fusion proteins, we established a pair of B2H counter-assays. Specifically, we were able to detect the 'self-interactions' of Hfq and $MS2^{CP}$, respectively, by testing the α-Hfq fusion protein in combination with a λCI-Hfq fusion protein and testing the λCI-$MS2^{CP}$ fusion protein in combination with an α-$MS2^{CP}$ fusion protein. In reporter cells containing the two Hfq fusion proteins, we observed an 11-fold stimulation of β-galactosidase activity over the basal activity level (measured in the presence of one or the other fusion protein; Figure 2B, top); similarly, in cells containing the two $MS2^{CP}$ fusion proteins, we observed an 8-fold stimulation of β-galactosidase activity over the basal activity level (Figure 2B, bot). The detection of these self-interactions is consistent with the known abilities of both Hfq and $MS2^{CP}$ to multimerize (43,44). We then tested the mutant fusion proteins (α-Hfq Q8A and λCI-$MS2^{CP}$ Y85S), each in combination with its WT partner and found that the magnitude of the self-interaction was unaltered compared with the WT/WT combination (Figure 2B). We conclude that the effects of Q8A in Hfq and Y85S in $MS2^{CP}$ on reporter gene expression as measured in the B3H assay reflect disruption of the Hfq–ChiX interaction, on the one hand, and the $MS2^{CP}$–$MS2^{hp}$ interaction, on the other. In the case of λCI substitution S45A, western blot analysis confirmed that the effect of this substitution on reporter gene expression in the B3H assay was not attributable to fusion protein destabilization, but instead reflected the disruptive effect on the λCI–operator interaction (Supplementary Figure S1).

α-Hfq multimerization contributes to Hfq–ChiX B3H interaction

Because Hfq functions as a hexamer, we hypothesized that the B3H complex consists of a hexameric assembly of α-Hfq subunits, of which one or two are functionally incorporated into RNAP. To test, explicitly, whether or not α-

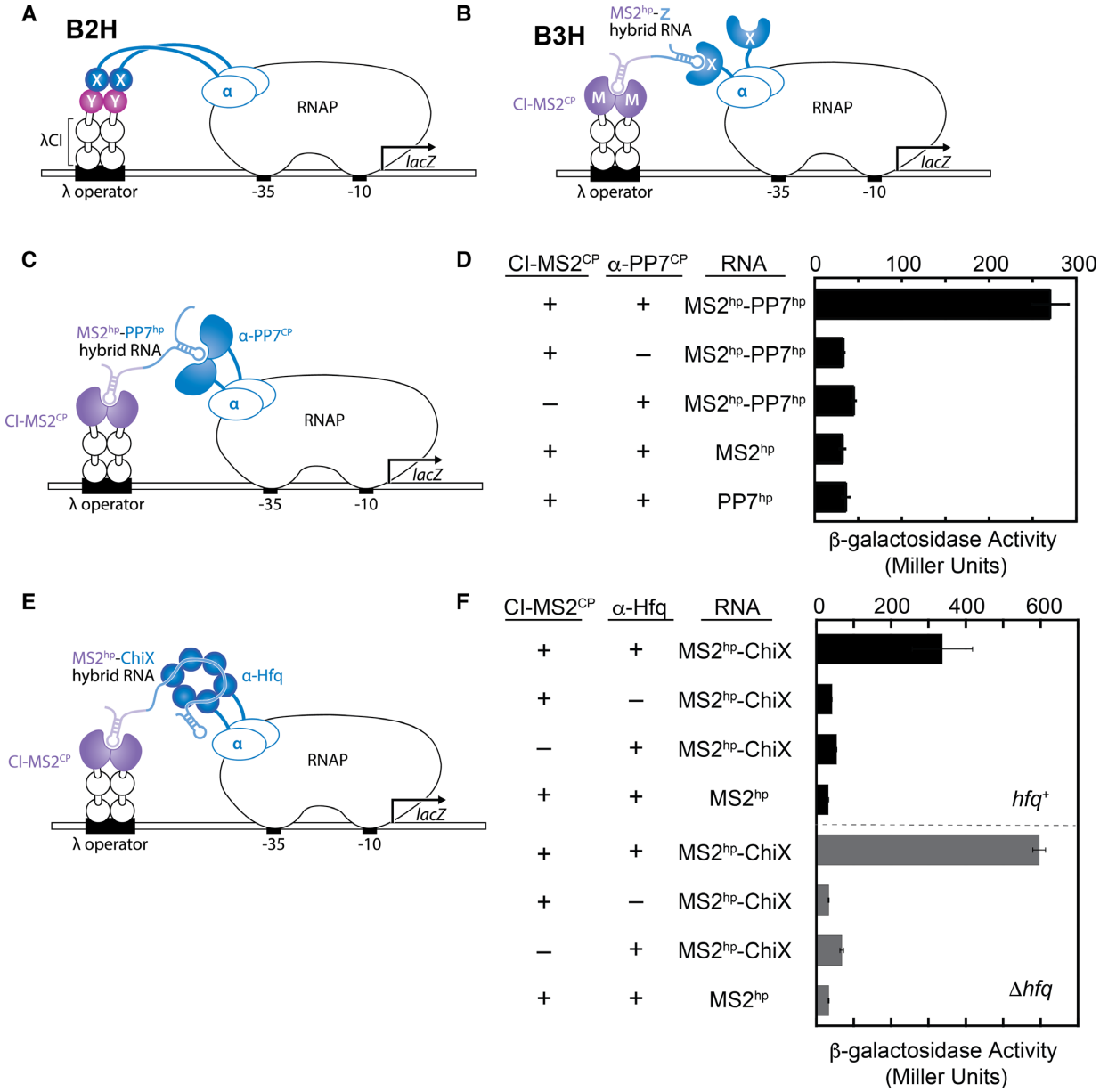

Figure 1. An *Escherichia coli* B3H interaction detects RNA–protein interactions. (**A**) Schematic showing bacterial B2H system. Interaction between protein moieties X and Y fused, respectively, to the N-terminal domain of the α subunit of RNAP (α-NTD) and to the bacteriophage λ CI protein (λCI) activates transcription from test promoter, which directs transcription of a *lacZ* reporter gene. The test promoter (p*lac*O_L2–62), which bears the λ operator O_L2 centered at position −62 relative to the transcription start site, is present on a single copy F' episome (33). (**B**) Schematic showing B3H system. Interaction between protein moiety X and RNA moiety Z fused, respectively, to the α-NTD and to the MS2 RNA hairpin ($MS2^{hp}$) activates transcription from the same test promoter used in (A). Two tandem copies of the $MS2^{hp}$ were present in all hybrid RNA constructs used in this study. For clarity, diagrams show only one hairpin. The RNA-binding moiety $MS2^{CP}$ is fused to λCI to tether the hybrid RNA ($MS2^{hp}$-Z) to the test promoter. Compatible plasmid vectors direct the synthesis of the two fusion proteins (both under the control of IPTG-inducible promoters) and the hybrid RNA (under the control of an arabinose-inducible promoter). Test promoter p*lac*O_L2–62 is the same as in (A). (**C**) Design of B3H system to detect interaction between $PP7^{CP}$ and $PP7^{hp}$. The λCI-$MS2^{CP}$ fusion protein and test promoter p*lac*O_L2–62 are the same as in (B). $PP7^{CP}$ is fused to the α-NTD. The fused protein moieties ($MS2^{CP}$ and $PP7^{CP}$) are bridged by the hybrid RNA ($MS2^{hp}$-$PP7^{hp}$) containing two tandem copies of each cognate RNA hairpin (diagram shows only one copy of each) followed by a *trpA* intrinsic terminator (not shown). (**D**) Results of β-galactosidase assays performed with reporter strain cells containing three compatible plasmids: one that encoded λCI (−) or the λCI-$MS2^{CP}$ fusion protein (+), another that encoded α (−) or the α-$PP7^{CP}$ fusion protein (+) and a third that encoded the hybrid RNA ($MS2^{hp}$–$PP7^{hp}$) or an RNA that contained only one tandem hairpin moiety ($MS2^{hp}$ or $PP7^{hp}$). The cells were grown in the presence of 0.2% arabinose and 5 μM IPTG (see Methods). (**E**) Design of B3H system to detect interaction between Hfq and the sRNA ChiX. The λCI-$MS2^{CP}$ fusion protein and test promoter p*lac*O_L2–62 are the same as in (B). Hfq is fused to the α-NTD and is depicted as a hexameric assembly, with two of the six subunits tethered directly to RNAP. The fused $MS2^{CP}$ moiety and the Hfq hexamer are bridged by hybrid RNA $MS2^{hp}$–ChiX (shown with the ChiX intrinsic terminator hairpin at the RNA 3′ end). (**F**) Results of β-galactosidase assays performed with *hfq*$^+$ (top) or Δ*hfq* (bottom) reporter strain cells containing three compatible plasmids: one that encoded λCI (−) or the λCI-$MS2^{CP}$ fusion protein (+), another that encoded α (−) or the α-Hfq fusion protein (+) and a third that encoded the hybrid RNA ($MS2^{hp}$–ChiX) or an RNA that contained only the $MS2^{hp}$ moiety. The cells were grown as in (D). Bar graphs show the averages of three independent measurements and standard deviations (D and F). All subsequent assays were performed in Δ*hfq* reporter strain cells unless otherwise noted.

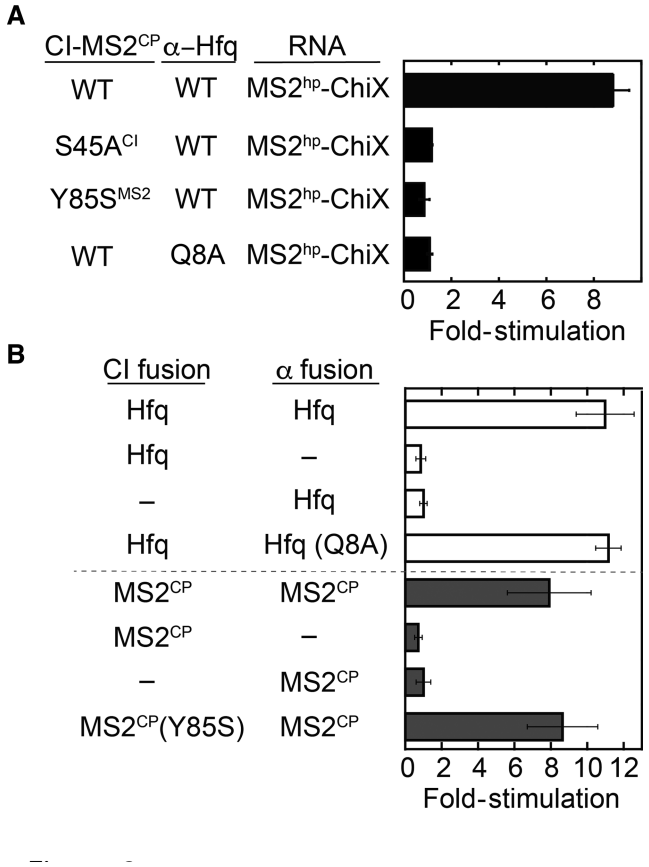

Figure 2. Effects of specific disruptive amino acid substitutions on B3H and B2H interactions. (**A**) Results of B3H assay. β-galactosidase assays were performed with Δ*hfq* reporter strain cells containing three compatible plasmids: one that encoded λCI or the λCI–$MS2^{CP}$ fusion protein (WT or the indicated mutant), another that encoded α or the α-Hfq fusion protein (WT or the indicated mutant) and a third that encoded the hybrid RNA ($MS2^{hp}$–ChiX) or an RNA that contained only the $MS2^{hp}$ moiety. The cells were grown in the presence of 0.2% arabinose and 5 μM IPTG (see 'Materials and Methods' section). (**B**) Results of B2H assays. Top: Hfq–Hfq interaction. β-galactosidase assays were performed with Δ*hfq* reporter strain cells containing two compatible plasmids: one that encoded λCI (–) or the λCI-Hfq fusion protein and another that encoded α (–) or the α-Hfq fusion protein (WT or the Q8A mutant). Bottom: $MS2^{CP}$–$MS2^{CP}$ interaction. β-galactosidase assays were performed with Δ*hfq* reporter strain cells containing two compatible plasmids: one that encoded λCI (–) or the λCI-$MS2^{CP}$ fusion protein (WT or the Y85S mutant) and another that encoded α (–) or the α-$MS2^{CP}$ fusion protein. In both cases, the cells were grown in the presence of 0.2% arabinose and 5 μM IPTG (see 'Materials and Methods' section). Bar graphs show the fold-stimulation over basal levels: that is, the β-galactosidase activity measured in the presence of all hybrid constructs divided by the activity of the highest negative control sample lacking one of the hybrid constructs (see 'Materials and Methods' section). Values shown are the averages and standard deviations of three independent measurements (A and B).

Hfq subunits that are incorporated into RNAP recruit additional Hfq subunits into the B3H complex, we examined the effect of α-Hfq substitution Q8A in reporter cells that did or did not contain chromosomally encoded Hfq (hfq^+ versus *Δhfq*). If α-Hfq subunits that are incorporated into RNAP do not recruit additional subunits to the complex, then the disruptive effect of the Q8A substitution on the B3H interaction should not be mitigated in the presence of WT chromosomally encoded Hfq. Conversely, if incorporated α-Hfq subunits recruit additional subunits to the complex, then the presence of WT chromosomally encoded Hfq might be expected to mitigate the effect of the Q8A substitution. Consistent with Hfq multimerization (presumably hexamer formation) at the test promoter, we found that the Q8A substitution was only mildly disruptive for the Hfq–ChiX B3H interaction when tested in hfq^+ reporter strain cells, as compared with *Δhfq* cells where the sole source of Hfq is the mutant α-Hfq fusion protein (Figure 3A).

In order to test whether or not α-Hfq multimerization is required for the Hfq–ChiX interaction detected in the B3H assay, we sought to identify a mutation that would disrupt the Hfq monomer–monomer interaction *in vivo*. Based on the structure of Hfq hexamers (43,45,46), we identified Met 53, a hydrophobic residue in the buried interface between Hfq monomers (Figure 3B), as a candidate residue that might be expected to contribute strongly to hexamerization. We chose to replace this methionine with a glutamate because burying a charged residue at a hydrophobic interface should be highly disfavored energetically. We first tested the effect of the M53E substitution on the B2H Hfq self-interaction and found, as expected, that when both fusion proteins (λCI-Hfq and α-Hfq) carried the substitution, the stimulation of reporter gene expression was nearly abolished (Figure 3C). In contrast, when only one of the fusion proteins carried the substitution, the Hfq self-interaction was maintained (Figure 3C), consistent with the expectation that under these circumstances the two fused Hfq moieties can pair in such a way that a fully WT interface is established (Supplementary Figure S2A and B). Moreover, this observation indicates that both mutant fusion proteins are well-folded and stable. Having thus shown that the α-Hfq M53E fusion protein is specifically defective for Hfq multimerization, we were in a position to evaluate the role of Hfq multimerization in the Hfq–ChiX B3H interaction. We found that substitution M53E abolished any detectable B3H interaction between Hfq and ChiX (Figure 3D), consistent with the hypothesis that B3H interaction between Hfq and ChiX depends on Hfq multimerization. As an additional control, we compared the intrinsic stabilities of α-Hfq and α-Hfq M53E; the results confirmed that the disruptive effect of the M53E substitution on the Hfq–ChiX interaction is not an indirect consequence of fusion protein destabilization (Supplementary Figure S2C).

α-Hfq supports sRNA function *in vivo*

With evidence for the formation of functionally relevant α-Hfq multimers (Figure 3A–D), we wished to assess whether or not the α-Hfq fusion protein can support sRNA function in a strain that contains no other source of Hfq. To do this, we employed an *in vivo* functional assay using single-copy reporters based on literature precedents (47). The reporters possess an IPTG-dependent promoter driving the transcription of the 5′ untranslated region (UTR) and first eight codons of an sRNA-regulated ORF fused in frame to the *lacZ* gene. Three *mRNA–lacZ* reporters were used: *sodB-lacZ, chiP-lacZ and eptB-lacZ*. These mRNAs are regulated by Hfq-dependent sRNAs RyhB, ChiX and MgrR, respectively (48–50). Expression of *lacZ* from each reporter increased several fold (3- to 9-fold) when an otherwise iso-

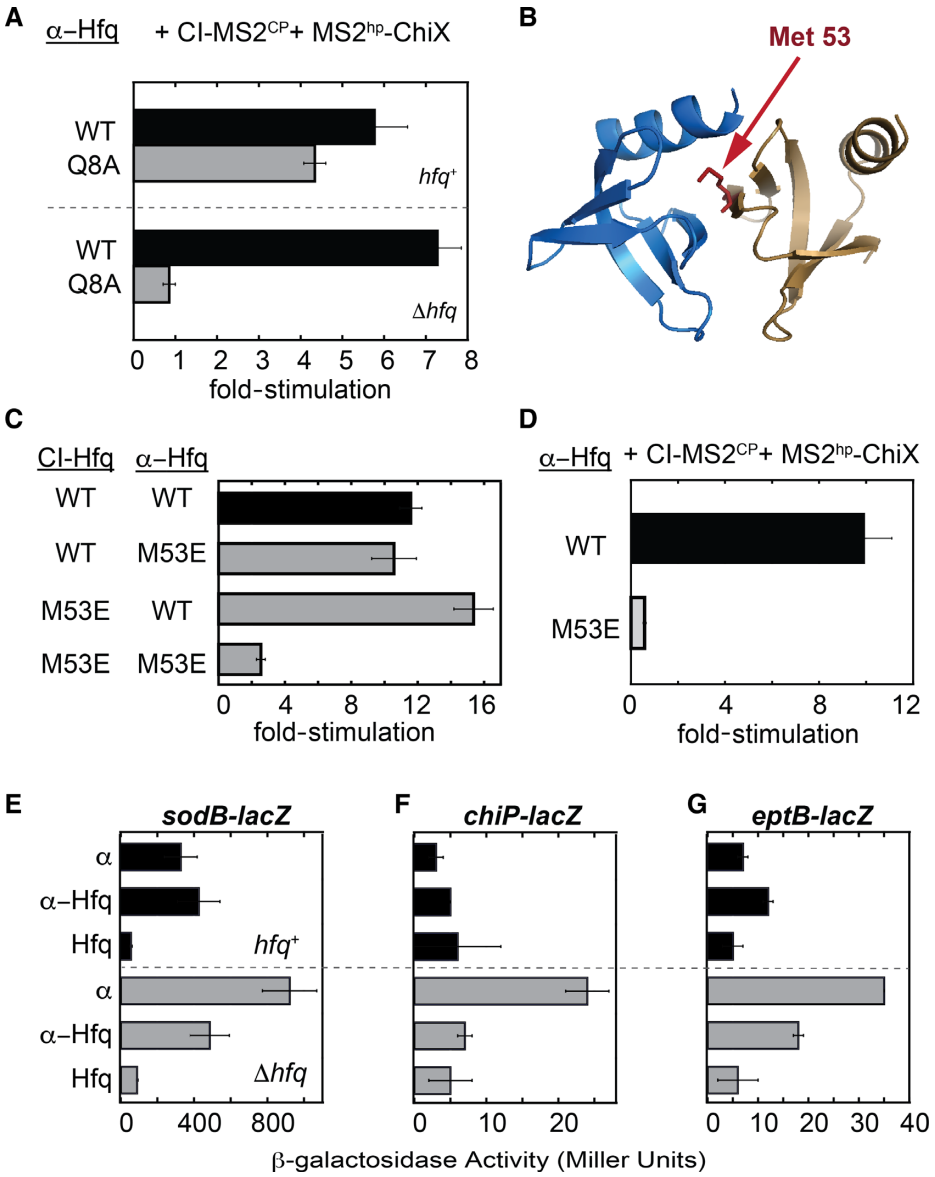

Figure 3. αNTD-Hfq fusion protein multimerizes in order to interact with MS2^{hp}–ChiX hybrid RNA and supports sRNA-mediated regulation of target mRNAs. (**A**) Results of B3H assay. β-galactosidase assays were performed with *hfq*$^{+}$ or Δ*hfq* reporter strain cells containing three compatible plasmids: one that encoded λCI or the λCI-MS2^{CP} fusion protein, another that encoded α or the α-Hfq fusion protein (WT or a Q8A mutant), and a third that encoded the hybrid RNA (MS2^{hp}–ChiX) or an RNA that contained only the MS2^{hp} moiety. The cells were grown in the presence of 0.2% arabinose and 5 μM IPTG (see 'Materials and Methods' section). The bar graph shows the fold-stimulation over basal levels (see Figure 2 legend) as the averages and standard deviations of three independent measurements. (**B**) Cartoon of Hfq structure, highlighting the location of residue Methionine 53 at the monomer–monomer interface. Each Hfq monomer is displayed as a ribbon diagram in either blue or gold and M53 is shown in red sticks. The figure was made from PDB ID: 4HT9 (46). (**C**) Results of B2H assay. β-galactosidase assays were performed with Δ*hfq* reporter strain cells containing two compatible plasmids: one that encoded λCI or the λCI-Hfq fusion protein (WT or an M53E mutant) and another that encoded α or the α-Hfq fusion protein (WT or the M53E mutant). To maintain consistent growth conditions between B3H and B2H assays, an empty pCDF vector (pKB822) was also present. Cells were grown in the presence of 0.2% arabinose and 5 μM IPTG (see 'Materials and Methods' section). The bar graph shows the fold-stimulation over basal levels as the averages and standard deviations of three independent measurements. (**D**) Results of B3H assays. β-galactosidase assays were performed with Δ*hfq* reporter strain cells containing three compatible plasmids: one that encoded λCI or the λCI-MS2^{CP} fusion protein, another that encoded α or the α-Hfq fusion protein (WT or an M53E mutant), and a third that encoded the hybrid RNA (MS2^{hp}–ChiX) or an RNA that contained only the MS2^{hp} moiety. The cells were grown in the presence of 0.2% arabinose and 5 μM IPTG (see 'Materials and Methods' section). The bar graph shows the fold-stimulation over basal levels as the averages and standard deviations of three independent measurements. (**E**–**G**) Effects of α-Hfq fusion protein on sRNA function *in vivo*. β-galactosidase assays were performed with *hfq*$^{+}$ or Δ*hfq* cells expressing a reporter in which the 5′UTR and first eight codons of (F) *eptB*, (G) *chiP* or (H) *sodB* were fused in frame to *lacZ*, under the control of an IPTG-inducible promoter. These reporters were present on a single copy F' episome. Reporter strain cells were transformed with a plasmid encoding α, the α-Hfq fusion protein or Hfq alone, also under the control of an IPTG-inducible promoter. The cells were grown in the presence of 5 μM IPTG to early stationary phase (see 'Materials and Methods' section). Bar graphs show average β-galactosidase values and standard deviations of three independent measurements.

genic reporter strain was deleted for *hfq* (Figure 3E–G, row 1 versus row 4), demonstrating that the expression of these mRNAs is Hfq-dependent under these assay conditions. In the *Δhfq* strains, overproduction of unfused WT Hfq (provided by a plasmid) caused *lacZ* expression from each reporter to decrease to approximately the level measured in the corresponding hfq^+ strain (*chiP* and *eptB*) or below (*sodB*) (Figure 3E–G, row 6 versus row 1). Overproduction of the α-Hfq fusion protein also resulted in decreased *lacZ* expression from each of the reporters (row 5 versus row 4), though not to the same extent as seen with WT Hfq (row 6). We conclude that α-Hfq has the ability to support sRNA function *in vivo*.

B3H assay detects interactions between *E. coli* Hfq and multiple sRNAs

Next, we sought to determine whether the B3H assay could detect additional Hfq–sRNA interactions. Specifically, we tested sRNAs OxyS, MgrR, McaS and RyhB. We observed a ≥2-fold increase in β-galactosidase activity with the OxyS, MgrR and McaS hybrid RNAs, but no increase with the RyhB hybrid RNA (Figure 4A, left), indicating that not all Hfq-dependent sRNAs interact detectably with Hfq in this system. Introduction of the Q8A substitution into the α-Hfq fusion protein abolished the B3H interactions of Hfq with OxyS, MgrR and McaS (Figure 4A, right), consistent with the expected disruptive effect of this substitution on each of these interactions. One possible explanation for our inability to detect an interaction between Hfq and RyhB is that the $MS2^{hp}$–RyhB hybrid RNA is poorly expressed. However, northern blotting using an oligonucleotide complementary to the $MS2^{hp}$ sequences common to all hybrid RNAs revealed that the intrinsic steady-state expression level of the $MS2^{hp}$–RyhB hybrid RNA (i.e. in the absence of α-Hfq and λCI-$MS2^{CP}$) was at least as high as any of the Hfq-interacting $MS2^{hp}$–sRNA fusions (Figure 4B), excluding this possible explanation.

Pilot screen to find mutations in Hfq that disrupt sRNA binding

Our findings suggest that our B3H system should facilitate genetic screening to identify mutations that affect the binding of a RNA-binding protein to its RNA ligand. As proof-of-principle, we sought to use the system to screen for Hfq mutations disrupting the Hfq-OxyS interaction. B3H reporter strain cells containing the λCI-$MS2^{CP}$ fusion protein and the $MS2^{hp}$–OxyS hybrid RNA were transformed with a PCR-mutagenized α-Hfq plasmid library and plated on appropriate indicator medium to enable a clear distinction between blue positive control colonies (containing the WT fusion proteins and the $MS2^{hp}$–OxyS hybrid RNA) and white negative control colonies (containing the WT fusion proteins, but lacking the $MS2^{hp}$–OxyS hybrid RNA; Supplementary Figure S3A). Among ∼1000 colonies screened, we identified 31 white or pale colonies, the phenotype expected for transformants that contained α-Hfq mutants that no longer interacted with the $MS2^{hp}$–OxyS hybrid RNA. To eliminate α-Hfq mutants that were misfolded and/or unstable, we performed a counter screen by using the B2H assay to assess the Hfq self-interaction. Specifically, plasmid DNA from the 31 candidate clones was pooled and used to transform reporter strain cells containing WT λCI-Hfq to identify blue colonies indicative of a robust self-interaction (Supplementary Figure S3B).

We identified eight α-Hfq mutants that passed both the primary screen and the counter screen, suggesting that the fused Hfq moieties were properly folded and the corresponding fusion proteins stably produced, but that the fused Hfq moieties were defective in their abilities to bind OxyS.

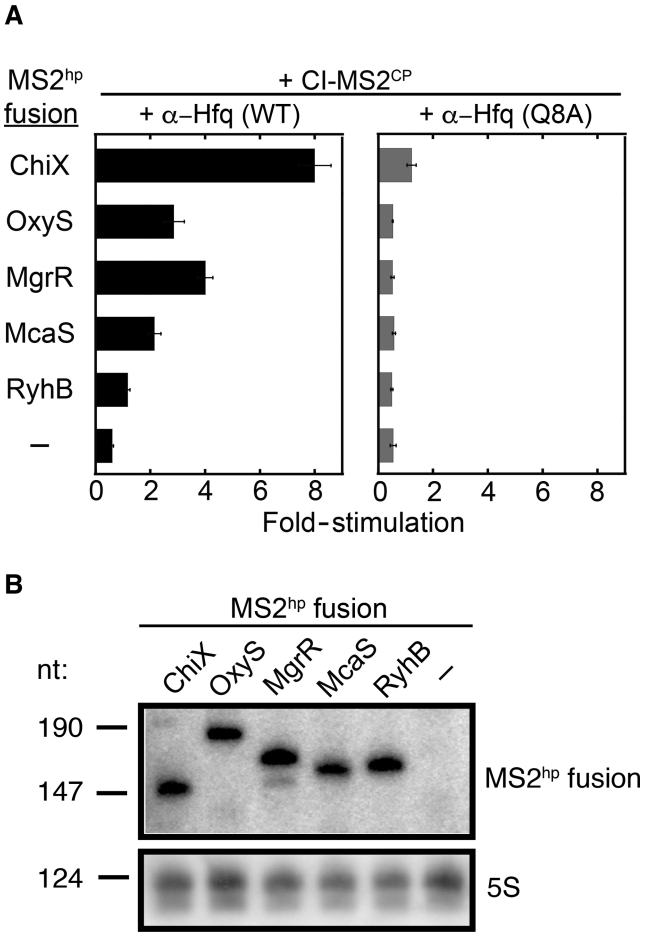

Figure 4. B3H assay detects multiple sRNA–Hfq interactions. (**A**) Results of B3H assays. β-galactosidase assays were performed with Δ*hfq* reporter strain cells containing three compatible plasmids: one that encoded λCI or the λCI-$MS2^{CP}$ fusion protein, another that encoded α or the α-Hfq fusion protein (WT or the Q8A mutant) and a third that encoded a hybrid RNA (the $MS2^{hp}$ moieties fused to ChiX, OxyS, MgrR, McaS or RyhB) or an RNA that contained only the $MS2^{hp}$ moiety (–). The cells were grown in the presence of 0.2% arabinose and 5 μM IPTG (see 'Materials and Methods' section). The bar graph shows the fold-stimulation over basal levels (see Figure 2 legend) as the averages and standard deviations of three independent measurements. (**B**) Results of northern blotting to assess steady state expression levels of hybrid RNAs. Total RNA was prepared from Δ*hfq* reporter strain cells containing three compatible plasmids: one that encoded λCI, another that encoded α and a third that encoded one of each of the $MS2^{hp}$–sRNA hybrid RNAs in (A) or only the $MS2^{hp}$ moiety (–). RNAs were detected either with an oligonucleotide probe that hybridizes to the $MS2^{hp}$ sequences shared by the hybrid RNAs or with an oligonucleotide probe that hybridizes to 5S rRNA as a loading control. Expected sizes of hybrid RNAs are: $MS2^{hp}$-ChiX 159 nt; $MS2^{hp}$-OxyS 192 nt; $MS2^{hp}$-MgrR 173 nt; $MS2^{hp}$-McaS 168 nt; $MS2^{hp}$-RyhB 169 nt; $MS2^{hp}$ alone ∼69 nt.

DNA sequence analysis revealed that each of these mutants bore a single amino acid substitution. Five of the eight affected residues (Q8, I30, F39, Y55 and H57) have been previously implicated in sRNA binding (40,51–53). Quantitative β-galactosidase assays indicated that mutations affecting these five residues abolished any detectable three-hybrid interaction between Hfq and OxyS and that mutations affecting residues not previously implicated in sRNA binding either abolished (L15) or strongly reduced (P10 and N13) the interaction of Hfq with OxyS (Figure 5A). To assess whether or not any of the substitutions specifically disrupted Hfq's interaction with OxyS as compared with other sRNAs, we tested the mutants for their abilities to interact with ChiX. All were defective and the pattern of the defects was very similar for OxyS and ChiX (Figure 5A and B), suggesting that these substitutions are generally disruptive for Hfq–sRNA interactions. Quantitative β-galactosidase assays also confirmed that each of these α-Hfq mutants maintained a near WT interaction with WT λCI-Hfq (Figure 5C), consistent with the results of the plate-based counterscreen. To uncover any potential defects in multimerization, we also tested the effect of each amino acid substitution on the Hfq self-interaction when both partners (α-Hfq and λCI-Hfq) were mutant (recall that the effect of the M53E substitution was apparent only when both interacting partners carried the substitution; Figure 3C). When tested in this manner, three of the eight substitutions (L15P, Y55C and H57R) caused a reduction in the Hfq self-interaction (Figure 5D, indicated by double dagger). Thus, it is possible that the effects of these three substitutions on the B3H interactions with OxyS and ChiX are partially or wholly due to destabilization of α-Hfq hexamers. Consistent with this possibility, these three residues (L15, Y55 and H57) are located close to the Hfq monomer–monomer interface; other affected residues map to the proximal (Q8, P10, N13 and F39) and distal (I30) faces of Hfq (Figure 5E and Supplementary Figure S4). We conclude that our tandem B3H/B2H screening strategy provides a facile method for identifying non-destabilizing Hfq mutations that disrupt its interaction with sRNA ligands.

DISCUSSION

In this work, we have established a B3H assay to detect RNA–protein interactions *in vivo*. Because it is based on transcription activation, this assay should be generalizable to any reporter system or selectable marker of interest. Several RNA–protein interactions have been used here to validate the assay: an interaction between the bacteriophage PP7 coat protein and its cognate RNA hairpin as well as interactions between *E. coli* Hfq and four of its partner sRNAs. The assay is sufficiently robust that we were able to perform a genetic screen to uncover both known and novel mutations in Hfq that compromise its ability to bind sRNAs.

Hfq–sRNA interactions detected with B3H assay

Our findings suggest that this B3H assay can detect the interaction of some, but not all, sRNAs with Hfq. Interestingly, all four sRNAs for which Hfq interactions were detected have been proposed to be 'Class II' sRNAs (ChiX, MgrR and McaS), or have significant Class II character (OxyS) based on a recent study (40). Class II RNAs are proposed to interact with the distal face of Hfq in addition to the proximal face, the classically defined interaction surface for sRNAs. It is possible that the geometry of this interaction is preferable for the B3H assay, or that Class II sRNAs are better able to compete with endogenous sRNAs for binding to the α-Hfq fusion protein (40). ChiX in particular has been shown to effectively compete with other sRNAs for Hfq binding, both *in vitro* and *in vivo* (36,37).

We do not know whether or not sRNA-mediated regulation of mRNA function can occur in the context of our B3H assembly. That is, we do not know if the RNAP-associated α-Hfq assembly can facilitate interaction between $MS2^{hp}$–sRNA hybrid RNAs and cognate target mRNAs. Because some Hfq-dependent sRNAs are degraded together with their mRNA targets (54), this process could in principle limit detection of specific Hfq–sRNA interactions using the B3H system. We note that although Hfq interacts in a dynamic fashion with its sRNA and mRNA ligands, catalyzing the functionally relevant base-pairing interactions between them ((55) and reviewed in (12)), our B3H system is evidently capable of capturing the initial binding of an sRNA to Hfq.

B3H and B2H assays permit genetic analysis of Hfq–sRNA and Hfq self-interactions

To facilitate screening for Hfq mutants with specific sRNA-binding defects, we established a B2H assay for detecting the interaction of Hfq with itself. As validation, we showed that replacement of M53, a conserved hydrophobic residue buried at the Hfq monomer–monomer interface (45), with a charged residue disrupted the Hfq self-interaction in our B2H assay. By using this B2H assay as a counter screen, we were able to discard mutations with general destabilizing effects. Moreover, the B2H assay also enabled us to distinguish mutations that did or did not affect the Hfq self-interaction (mutations with effects on the Hfq self-interaction manifested a B2H phenotype only when present in both interacting partners; see Figure 3C and Supplementary Figure S2B). *In vitro*, Hfq monomers undergo a cooperative transition to multimers with a K_D of ∼1 μM (56). Two mutations from our screen that disrupted the Hfq self-interaction as detected in the B2H assay (Y55C and H57R) occurred at amino acid positions where mutations have been shown previously to reduce Hfq multimerization using semi-denaturing gel electrophoresis (42,56). In contrast, the Q8A proximal-face mutation, which has also been shown to favor Hfq monomers when analyzed by semi-denaturing gel electrophoresis (42,56), did not perturb the B2H Hfq self-interaction in this study. This difference may result from the B2H assay being conducted in native conditions *in vivo* without the need for cell lysis and/or gel electrophoresis.

Of the eight amino acid positions identified in our screen for Hfq mutants with defects in binding the OxyS sRNA, mutations at five of these positions have been shown previously to disrupt sRNA binding *in vivo*: Q8 and F39 on the proximal face, I30 on the distal face, and Y55 and H57 near the pore (40,51–53). Our B3H mutant screen also im-

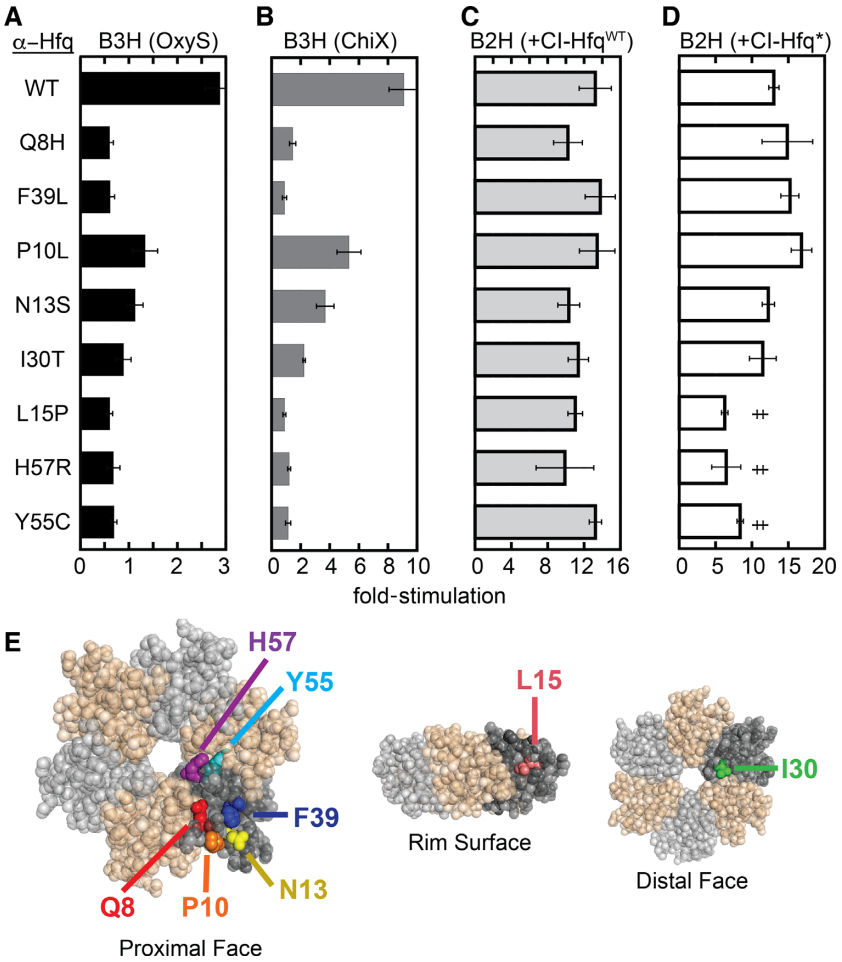

Figure 5. Pilot screen to identify mutations that alter the strength of Hfq–sRNA interaction. (**A** and **B**) Results of B3H assays. β-galactosidase assays were performed with Δ*hfq* reporter strain cells containing three compatible plasmids: one that encoded λCI or the λCI-MS2^{CP} fusion protein, another that encoded α or the α-Hfq fusion protein (WT or the indicated mutant) and a third that encoded the hybrid RNA (A: MS2^{hp}–OxyS, B: MS2^{hp}–ChiX) or an RNA that contained only the MS2^{hp} moiety. The cells were grown in the presence of 0.2% arabinose and 5 μM IPTG (see 'Materials and Methods' section). Bar graphs show the fold-stimulation over basal levels (see Figure 2 legend) as the averages and standard deviations of three independent measurements. (**C** and **D**) Results of B2H assays. β-galactosidase assays were performed with Δ*hfq* reporter strain cells containing three compatible plasmids: one that encoded λCI or the CI-Hfq fusion protein (C: WT, D: WT or the indicated mutant), another that encoded α or the α-Hfq fusion protein (WT or the indicated mutant) and a third that encoded an RNA that contained only the MS2^{hp} moiety. The cells were grown in the presence of 0.2% arabinose and 5 μM IPTG (see 'Materials and Methods' section). Bar graphs show the fold-stimulation over basal levels as the averages and standard deviations of three independent measurements. Substitutions that cause a reduced self-interaction are indicated with a double dagger. (**E**) Space-filling representation of Hfq hexamer structure (PDB ID: 4HT9) (46). Individual Hfq monomers are shown in gold, silver or dark gray (a single subunit). Residues that were identified in the screen are shown in colored spheres on a single monomer (dark gray), viewed from the proximal face (Q8, P10, N13, F39, Y55, H57), rim surface (L15) or distal face (I30).

plicated several previously uncharacterized Hfq residues in contributing to sRNA binding. Residue N13, on Hfq's proximal face, was observed to hydrogen bond to two sRNA uridines in a co-crystal structure with the sRNA RydC (57), consistent with our finding that an Hfq-N13S mutant was deficient in binding both OxyS and ChiX in our B3H assay. Residue P10 is on Hfq's proximal face, located in the same α-helix as Q8 and N13, and may contribute to sRNA binding in part through an effect on the conformation of Q8 (Supplementary Figure S4B). Residue L15 is buried in the Hfq crystal structure and likely contributes to sRNA binding indirectly through an effect on Hfq structure and multimerization, consistent with the disruption of the Hfq self-interaction by substitution L15P in our B2H assay. There has been considerable interest recently in classifying sRNAs based on their interaction surfaces with Hfq, and it appears from both *in vitro* and *in vivo* methods that not all sRNAs make use of the same Hfq binding surfaces (40,41). The B3H assay developed here should, in principle, allow for appropriate screening and counter screening to identify residues that preferentially contribute to the interaction of Hfq with one sRNA relative to another.

Prospect

The B3H assay established here will expand the tools currently available to investigate RNA–protein interactions (4,5,7–10,34,58) and complements previous techniques in ways that should extend their utility. As an alternative *in vivo* method to three-hybrid assays in yeast (1,2,8,22), our

E. coli-based system offers high transformation efficiency as well as a distinct cellular machinery and environment to produce fusion proteins and hybrid RNAs. In particular, unlike yeast RNAP III, which is used to produce hybrid RNAs in the most commonly used yeast three-hybrid systems, *E. coli* RNAP can transcribe U-rich stretches and recognizes bacterial intrinsic terminators (27). Here, the MS2 hairpins have been fused to the 5′ end of sRNAs in order to maintain their native 3′ intrinsic terminators, which contribute to the binding interactions of many sRNAs with Hfq (59). We anticipate that the B3H assay could be applied to genetic screens with genomic libraries to identify novel RNA–protein interactions. This assay also enables the use of genetic approaches to isolate mutants that can be helpful mechanistic tools for further studies. The B3H assay thus has the potential to be an advantageous tool in the study of Hfq–sRNA interactions from diverse bacteria and to be broadly applicable to RNA–protein interactions from bacteria and other organisms.

SUPPLEMENTARY DATA

Supplementary Data are available at NAR Online.

ACKNOWLEDGEMENTS

We thank members of the laboratory and Simon Dove for comments on the manuscript, advice and discussion. We thank Marvin Wickens for providing plasmids, Susan Gottesman and Gigi Storz for helpful discussions and for providing plasmids, and Renate Hellmiss for artwork.

FUNDING

National Institutes of Health [GM044025 to A.H., FGM102999 to K.E.B.]. Funding for open access charge: unrestricted funds.
Conflict of interest statement. None declared.

REFERENCES

1. SenGupta,D.J., Zhang,B., Kraemer,B., Pochart,P., Fields,S. and Wickens,M. (1996) A three-hybrid system to detect RNA-protein interactions in vivo. *Proc. Natl. Acad. Sci. U.S.A.*, **93**, 8496–8501.
2. Putz,U., Skehel,P. and Kuhl,D. (1996) A tri-hybrid system for the analysis and detection of RNA–protein interactions. *Nucleic Acids Res.*, **24**, 4838–4840.
3. Zhang,A., Wassarman,K.M., Rosenow,C., Tjaden,B.C., Storz,G. and Gottesman,S. (2003) Global analysis of small RNA and mRNA targets of Hfq. *Mol. Microbiol.*, **50**, 1111–1124.
4. Sittka,A., Lucchini,S., Papenfort,K., Sharma,C.M., Rolle,K., Binnewies,T.T., Hinton,J.C.D. and Vogel,J. (2008) Deep sequencing analysis of small noncoding RNA and mRNA targets of the global post-transcriptional regulator, Hfq. *PLoS Genet.*, **4**, e1000163.
5. Said,N., Rieder,R., Hurwitz,R., Deckert,J., Urlaub,H. and Vogel,J. (2009) In vivo expression and purification of aptamer-tagged small RNA regulators. *Nucleic Acids Res.*, **37**, e133.
6. Lorenz,C., Gesell,T., Zimmermann,B., Schoeberl,U., Bilusic,I., Rajkowitsch,L., Waldsich,C., Haeseler,Von, A. and Schroeder,R. (2010) Genomic SELEX for Hfq-binding RNAs identifies genomic aptamers predominantly in antisense transcripts. *Nucleic Acids Res.*, **38**, 3794–3808.
7. Zimmermann,B., Bilusic,I., Lorenz,C. and Schroeder,R. (2010) Genomic SELEX: a discovery tool for genomic aptamers. *Methods*, **52**, 125–132.
8. Martin,F. (2012) Fifteen years of the yeast three-hybrid system: RNA–protein interactions under investigation. *Methods*, **58**, 367–375.
9. Faner,M.A. and Feig,A.L. (2013) Identifying and characterizing Hfq–RNA interactions. *Methods*, **63**, 144–159.
10. Wang,T., Xiao,G., Chu,Y., Zhang,M.Q., Corey,D.R. and Xie,Y. (2015) Design and bioinformatics analysis of genome-wide CLIP experiments. *Nucleic Acids Res.*, **43**, 5263–5274.
11. Smirnov,A., Förstner,K.U., Holmqvist,E., Otto,A., Günster,R., Becher,D., Reinhardt,R. and Vogel,J. (2016) Grad-seq guides the discovery of ProQ as a major small RNA-binding protein. *Proc. Natl. Acad. Sci. U.S.A.*, **113**, 11591–11596.
12. Vogel,J. and Luisi,B.F. (2011) Hfq and its constellation of RNA. *Nat. Rev. Microbiol.*, **9**, 578–589.
13. Gottesman,S. and Storz,G. (2011) Bacterial small RNA regulators: versatile roles and rapidly evolving variations. *Cold Spring Harbor Perspect. Biol.*, **3**, a003798.
14. Updegrove,T.B., Zhang,A. and Storz,G. (2016) Hfq: the flexible RNA matchmaker. *Curr. Opin. Microbiol.* **30**, 133–138.
15. Carmichael,G.G., Weber,K., Niveleau,A. and Wahba,A.J. (1975) The host factor required for RNA phage Qβ RNA replication in vitro. Intracellular location, quantitation, and purification by polyadenylate-cellulose chromatography. *J. Biol. Chem.*, **250**, 3607–3612.
16. Møller,T., Franch,T., Højrup,P., Keene,D.R., Bächinger,H.P., Brennan,R.G. and Valentin-Hansen,P. (2002) Hfq: a bacterial Sm-like protein that mediates RNA-RNA interaction. *Mol. Cell*, **9**, 23–30.
17. Sun,X., Zhulin,I. and Wartell,R.M. (2002) Predicted structure and phyletic distribution of the RNA-binding protein Hfq. *Nucleic Acids Res.*, **30**, 3662–3671.
18. Sobrero,P. and Valverde,C. (2012) The bacterial protein Hfq: much more than a mere RNA-binding factor. *Crit. Rev. Microbiol.*, **38**, 276–299.
19. Wagner,E.G.H. and Romby,P. (2015) Small RNAs in bacteria and archaea: who they are, what they do, and how they do it. *Adv. Genet.*, **90**, 133–208.
20. Bossi,L., Schwartz,A., Guillemardet,B., Boudvillain,M. and Figueroa-Bossi,N. (2012) A role for Rho-dependent polarity in gene regulation by a noncoding small RNA. *Genes Dev.*, **26**, 1864–1873.
21. Sedlyarova,N., Shamovsky,I., Bharati,B.K., Epshtein,V., Chen,J., Gottesman,S., Schroeder,R. and Nudler,E. (2016) sRNA-mediated control of transcription termination in *E. coli*. *Cell*, **167**, 111–121.
22. Hook,B., Bernstein,D., Zhang,B. and Wickens,M. (2005) RNA-protein interactions in the yeast three-hybrid system: affinity, sensitivity, and enhanced library screening. *RNA*, **11**, 227–233.
23. Datsenko,K.A. and Wanner,B.L. (2000) One-step inactivation of chromosomal genes in Escherichia coli K-12 using PCR products. *Proc. Natl. Acad. Sci. U.S.A.*, **97**, 6640–6645.
24. Baba,T., Ara,T., Hasegawa,M., Takai,Y., Okumura,Y., Baba,M., Datsenko,K.A., Tomita,M., Wanner,B.L. and Mori,H. (2006) Construction of Escherichia coli K-12 in-frame, single-gene knockout mutants: the Keio collection. *Mol. Syst. Biol.*, **2**, 1–11.
25. Whipple,F.W. (1998) Genetic analysis of prokaryotic and eukaryotic DNA-binding proteins in Escherichia coli. *Nucleic Acids Res.*, **26**, 3700–3706.
26. Nickels,B.E., Roberts,C.W., Sun,H., Roberts,J.W. and Hochschild,A. (2002) The σ(70) subunit of RNA polymerase is contacted by the λQ antiterminator during early elongation. *Mol. Cell*, **10**, 611–622.
27. Bernstein,D.S., Buter,N., Stumpf,C. and Wickens,M. (2002) Analyzing mRNA-protein complexes using a yeast three-hybrid system. *Methods*, **26**, 123–141.
28. Macías,S., Bragulat,M., Tardiff,D.F. and Vilardell,J. (2008) L30 binds the nascent RPL30 transcript to repress U2 snRNP recruitment. *Mol. Cell*, **30**, 732–742.
29. Nickels,B.E. (2009) Genetic assays to define and characterize protein–protein interactions involved in gene regulation. *Methods*, **47**, 53–62.
30. Goldman,S.R., Nair,N.U., Wells,C.D., Nickels,B.E. and Hochschild,A. (2015) The primary σ factor in Escherichia coli can access the transcription elongation complex from solution in vivo. *Elife*, **4**,e10514.
31. Dove,S.L., Joung,J.K. and Hochschild,A. (1997) Activation of prokaryotic transcription through arbitrary protein-protein contacts. *Nature*, **386**, 627–630.

32. Dove,S.L. and Hochschild,A. (1998) Use of artificial activators to define a role for protein-protein and protein-DNA contacts in transcriptional activation. *Cold Spring Harb. Symp. Quant. Biol.*, **63**, 173–180.
33. Deaconescu,A.M., Chambers,A.L., Smith,A.J., Nickels,B.E., Hochschild,A., Savery,N.J. and Darst,S.A. (2006) Structural basis for bacterial transcription-coupled DNA repair. *Cell*, **124**, 507–520.
34. Gelderman,G., Sivakumar,A., Lipp,S. and Contreras,L. (2015) Adaptation of Tri-molecular fluorescence complementation allows assaying of regulatory Csr RNA-protein interactions in bacteria. *Biotechnol. Bioeng.*, **112**, 365–375.
35. Lim,F., Downey,T.P. and Peabody,D.S. (2001) Translational repression and specific RNA binding by the coat protein of the Pseudomonas phage PP7. *J. Biol. Chem.*, **276**, 22507–22513.
36. Moon,K. and Gottesman,S. (2011) Competition among Hfq-binding small RNAs in Escherichia coli. *Mol. Microbiol.*, **82**, 1545–1562.
37. Małecka,E.M., Stróżecka,J., Sobańska,D. and Olejniczak,M. (2015) Structure of bacterial regulatory RNAs determines their performance in competition for the chaperone protein Hfq. *Biochemistry*, **54**, 1157–1170.
38. Hochschild,A. and Ptashne,M. (1986) Homologous interactions of lambda repressor and lambda Cro with the lambda operator. *Cell*, **44**, 925–933.
39. Johansson,H.E., Dertinger,D., LeCuyer,K.A., Behlen,L.S., Greef,C.H. and Uhlenbeck,O.C. (1998) A thermodynamic analysis of the sequence-specific binding of RNA by bacteriophage MS2 coat protein. *Proc. Natl. Acad. Sci. U.S.A.*, **95**, 9244–9249.
40. Schu,D.J., Zhang,A., Gottesman,S. and Storz,G. (2015) Alternative Hfq-sRNA interaction modes dictate alternative mRNA recognition. *EMBO J.*, **34**, 2557–2573.
41. Updegrove,T.B. and Wartell,R.M. (2011) The influence of Escherichia coli Hfq mutations on RNA binding and sRNA·mRNA duplex formation in rpoS riboregulation. *Biochim. Biophys. Acta*, **1809**, 532–540.
42. Zhang,A., Schu,D.J., Tjaden,B.C., Storz,G. and Gottesman,S. (2013) Mutations in interaction surfaces differentially impact E. coli Hfq association with small RNAs and their mRNA targets. *J. Mol. Biol.*, **425**, 3678–3697.
43. Schumacher,M.A., Pearson,R.F., Møller,T., Valentin-Hansen,P. and Brennan,R.G. (2002) Structures of the pleiotropic translational regulator Hfq and an Hfq-RNA complex: a bacterial Sm-like protein. *EMBO J.*, **21**, 3546–3556.
44. Valegård,K., Murray,J.B., Stockley,P.G., Stonehouse,N.J. and Liljas,L. (1994) Crystal structure of an RNA bacteriophage coat protein-operator complex. *Nature*, **371**, 623–626.
45. Moskaleva,O., Melnik,B., Gabdulkhakov,A., Garber,M., Nikonov,S., Stolboushkina,E. and Nikulin,A. (2010) The structures of mutant forms of Hfq from Pseudomonas aeruginosa reveal the importance of the conserved His57 for the protein hexamer organization. *Acta Crystallogr. Sect. F Struct. Biol. Cryst. Commun.*, **66**, 760–764.
46. Wang,W., Wang,L., Wu,J., Gong,Q. and Shi,Y. (2013) Hfq-bridged ternary complex is important for translation activation of rpoS by DsrA. *Nucleic Acids Res.*, **41**, 5938–5948.
47. Mandin,P. and Gottesman,S. (2009) A genetic approach for finding small RNAs regulators of genes of interest identifies RybC as regulating the DpiA/DpiB two-component system. *Mol. Microbiol.*, **72**, 551–565.
48. Massé,E. and Gottesman,S. (2002) A small RNA regulates the expression of genes involved in iron metabolism in Escherichia coli. *Proc. Natl. Acad. Sci. U.S.A.*, **99**, 4620–4625.
49. Figueroa-Bossi,N., Valentini,M., Malleret,L. and Bossi,L. (2009) Caught at its own game: regulatory small RNA inactivated by an inducible transcript mimicking its target. *Genes Dev.*, **23**, 2004–2015.
50. Moon,K. and Gottesman,S. (2009) A PhoQ/P-regulated small RNA regulates sensitivity of Escherichia coli to antimicrobial peptides. *Mol. Microbiol.*, **74**, 1314–1330.
51. Mikulecky,P.J., Kaw,M.K., Brescia,C.C., Takach,J.C., Sledjeski,D.D. and Feig,A.L. (2004) Escherichia coli Hfq has distinct interaction surfaces for DsrA, rpoS and poly(A) RNAs. *Nat. Struct. Mol. Biol.*, **11**, 1206–1214.
52. Sun,X. and Wartell,R.M. (2006) Escherichia coli Hfq binds A18 and DsrA domain II with similar 2:1 Hfq6/RNA stoichiometry using different surface sites. *Biochemistry*, **45**, 4875–4887.
53. Updegrove,T., Wilf,N., Sun,X. and Wartell,R.M. (2008) Effect of Hfq on RprA-rpoS mRNA pairing: Hfq-RNA binding and the influence of the 5′ rpoS mRNA leader region. *Biochemistry*, **47**, 11184–11195.
54. Masse,E. (2003) Coupled degradation of a small regulatory RNA and its mRNA targets in Escherichia coli. *Genes Dev.*, **17**, 2374–2383.
55. Fender,A., Elf,J., Hampel,K., Zimmermann,B. and Wagner,E.G.H. (2010) RNAs actively cycle on the Sm-like protein Hfq. *Genes Dev.*, **24**, 2621–2626.
56. Panja,S. and Woodson,S.A. (2012) Hexamer to monomer equilibrium of E. coli Hfq in solution and its impact on RNA annealing. *J. Mol. Biol.*, **417**, 406–412.
57. Dimastrogiovanni,D., Fröhlich,K.S., Bandyra,K.J., Bruce,H.A., Hohensee,S., Vogel,J. and Luisi,B.F. (2014) Recognition of the small regulatory RNA RydC by the bacterial Hfq protein. *Elife*, **3**, 7901–7919.
58. Zhou,Y., Asahara,H., Schneider,N., Dranchak,P., Inglese,J. and Chong,S. (2014) Engineering bacterial transcription regulation to create a synthetic in vitro two-hybrid system for protein interaction assays. *J. Am. Chem. Soc.*, **136**, 14031–14038.
59. Sauer,E. and Weichenrieder,O. (2011) Structural basis for RNA 3'-end recognition by Hfq. *Proc. Natl. Acad. Sci. U.S.A.*, **108**, 13065–13070.